ChemComm

Guest-Dependent Bond Flexibility in UiO-66, a "Stable" MOF

Journal:	*ChemComm*
Manuscript ID	CC-COM-10-2022-005895.R1
Article Type:	Communication

COMMUNICATION

Guest-Dependent Bond Flexibility in UiO-66, a "Stable" MOF

Kevin Fabrizio,[a] Anastasia B. Andreeva,[a] Kentaro Kadota,[a] Amanda J. Morris [b] and Carl K. Brozek *[a]

Received 00th January 20xx,
Accepted 00th January 20xx

DOI: 10.1039/x0xx00000x

We report "flexibility constants"—a conceptual analog to metal-ligand stability constants, of UiO-66, the prototypical "stable" MOF, across a wide temperature range in both vacuum and in the presence of typical guest solvents. With these data, we extract key thermodynamic parameters governing the reversible bond equilibrium and demonstrate that guest molecules strongly favor the reversible dissociation of MOF metal-linker bonds.

Labile metal-ligand bonds drive important phenomena of both molecules and materials. In molecules, labile bonding gives rise to ligand exchange and the creation of open metal sites that enable catalysis,[1] whereas in materials, they cause vibronic interactions that strongly influence myriad magnetic, optical, and electronic properties.[2] Polaronic charge transport, Stokes shifts caused by self-trapped excitons, and structural phase changes induced by Peierls distortions exemplify the important role of structural dynamics. Soft modes comprise a special family of dynamic interactions, whereby particular vibrations trigger phase transitions by displacing atomic positions from one phase into the positions of the other phase.[3] The melting mechanism of many materials, for instance, involves vibrations that exceed the Lindemann ratio between the atomic displacement of a vibration and the nearest-neighbor distances that otherwise remains constant at around 0.1 for many stable phases.[4] While soft modes, and vibronic interactions in general, have been intensely studied for conventional solid-state materials, such as binary lattice semiconductors, their role in materials with more complex compositions remains an open frontier. For example, recent studies reveal that vibronic interactions explain important emergent properties of hybrid perovskites.[5,6]

Despite crystal structures that suggest rigid and static bonding, recent evidence has shown that metal-linker bonds in metal-organic frameworks (MOFs) are dynamic. We demonstrated through variable-temperature diffuse reflectance Fourier transform spectroscopy (VT-DRIFTS) that metal carboxylate and metal-azolate bonds in many common MOFs exist in an equilibrium between tightly and weakly bound configurations, as shown in **Scheme 1**.[7,8] As a result, the MOF bonding environment straddles two shallow potential-energy surfaces that shifts towards bond dissociation at high temperatures. The vibrations associated with these dynamic bonds exhibit the hallmark characteristics of soft modes, i.e., frequencies that redshift close to T_c of a phase transition, due to the vibration dissipating its energy to the lattice through anharmonic coupling. Dynamic metal linker bonds help explain many curious MOF properties.[9,10] For example, we demonstrated that the metal-triazolate bonds in the isostructural family of MOFs termed M(1,2,3-triazolate)$_2$ (M = Mn, Fe, Co, Cu, Zn, Cd) are labile and consequently serve as soft modes that trigger the unusually cooperative spin crossover transition in the Fe variant and the structural phase change in the Cu analog.[8] Dynamic bonding would also explain the ability of MOFs to undergo post-synthetic linker and cation exchange.[11–13] Labile metal-linker bonding could also explain how MOFs with metal sites that seem coordinatively saturated catalyze chemical transformations that require open metal sites.[14–16] The equilibrium constants of the reversible binding and unbinding of metal-linker bonds, termed stability constants, offer a quantitative measure of the microscopic aspects of bond dynamics. Previously, we reported a thermodynamic parameter akin to stability constants, defined

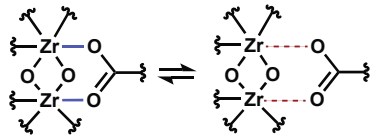

Scheme 1: A portion of the UiO-66 metal node, illustrating the dynamic equilibrium between ensembles of Zr-linker species existing as either tightly or loosely bound states.

[a] *Department of Chemistry and Biochemistry, Material Science Institute, University of Oregon, Eugene, OR 97403, United States*
[b] *Department of Chemistry, Virginia Tech, Blacksburg, VA 24060, United States*
Electronic Supplementary Information (ESI) available: [details of any supplementary information available should be included here]. See DOI: 10.1039/x0xx00000x

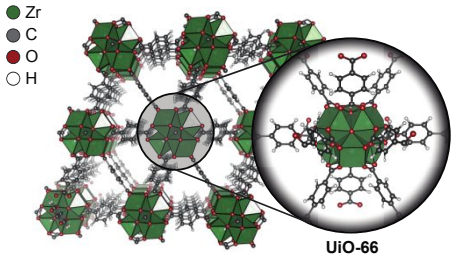

Figure 1: Representation of the crystallographic structure of UiO-66 prior to dehydration. The Zr-oxo node is highlighted.

as the ratio of "tight" and "loose" states as shown in Scheme 1. This quantity, which we term "flexibility constants", *X*, represent a thermodynamic equilibrium bonding mixture, *X* =([tight]/[loose]), as opposed to an equilibrium constant for the formation/dissociation of bonds, as for stability constants. Previous analysis of VT-DRIFTS data revealed that Cu_3(1,3,5-benzene tricarboxylate)$_2$, (CuBTC), the prototypical carboxylate MOF, and *M*(1,2,3-triazolate)$_2$ exhibit surprisingly small flexibility constants given the absence of solvent, and compared favorably to stability constants of molecular analogs.[17]

Here, we report the flexibility constants of UiO-66 ($Zr_6O_4OH_4$(1,4-benzenedicarboxylate)$_6$), a particularly "stable" MOF, extract thermodynamic parameters of the dynamic bonding equilibrium through a modified van't Hoff analysis designed for phase change systems, and show that the material is surprisingly dynamic.[18] These values provide a framework for understanding the chemical stability of MOFs, and for predicting and rationalizing behavior that involves dynamic bonding. Furthermore, these results reveal the sensitivity of the metal-linker dynamics to guest molecules, providing microscopic insight into the bonding equilibrium, and reveal an unexpected but important guest-host interaction relevant to the use of MOFs in gas capture and separation technologies.

The unusual pH- and water-stability of UiO-66 and related MOFs with zirconium oxo clusters has been attributed to robust Zr-O bonds, and yet our previous analysis hinted at metal-linker bond dynamics comparable to MOF-5 and other less stable MOFs. In a prior report, redshifting carboxylate stretches were evidenced by VT-DRIFTs for these and other common MOFs and were interpreted as thermal population of an ensemble of "loose" states that could be reversibly cycled, suggesting an equilibrium process akin to phase changes.[7] The red-shift slopes, χ, provided a quantitative measure of the "softness" of the carboxylate stretches, with steeper slopes indicating weaker bonding. Whereas MOF-5 displayed an asymmetric χ of –0.02 cm^{-1}/K, UiO-66 showed a comparable slope of –0.015 cm^{-1}/K, also consistent with the other surveyed carboxylate MOFs. Given the apparent discrepancy between the chemical stability of UiO-66 and evidence for dynamic Zr-O bonding, we reinvestigated the thermodynamic details of metal-linker lability in UiO-66 in comparison to less stable carboxylate MOFs.

Following a modified procedure,[19] bulk powder of UiO-66 was prepared, washed, and activated prior to analysis. **Figure 1** depicts the octahedral Zr-oxo clusters held together by Zr-carboxylate moieties at the focus of this report. To interrogate the lability and thermodynamics aspects of the Zr-linker bonding in UiO-66, we employed VT-DRIFTS. **Figure 2** summarizes the temperature dependence of the asymmetric carboxylate stretch of UiO-66 under dynamic vacuum and in air. **Figure 2a** shows the baseline-subtracted VT-DRIFTS spectra of UiO-66 collected between 294 K and 473 K under dynamic vacuum. The peak maxima redshift from 1589 cm^{-1} to 1586 cm^{-1} over this temperature range, consistent with a previous report that the Zr-carboxylate bonds weaken at higher temperatures by favoring the "loose" state conformation in a dynamic bond equilibrium.[7] Interestingly, the full-width-at-half-maximum (FWHM) values of the asymmetric stretch decreases across the measured temperature range (294 – 473K, Figure S6). Based on our earlier work, the observation of an increase and decrease in FWHM across low (< 294 K) and high (> 294 K) temperatures

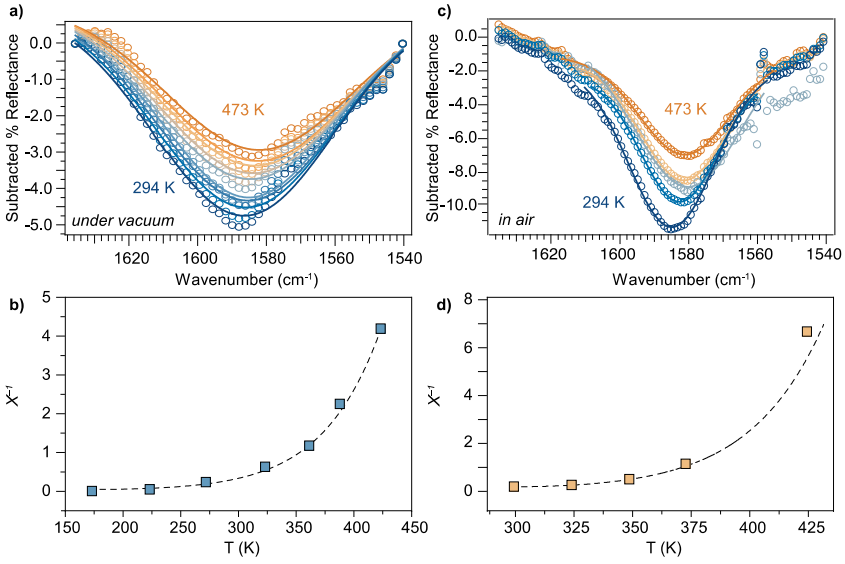

Figure 2: (a) Subtracted reflectance VT-DRIFTS of the UiO-66 asymmetric stretch under dynamic vacuum. **(b)** Modified van't Hoff plot of the asymmetric stretch of UiO-66 under dynamic vacuum. **(c)** Subtracted reflectance VT-DRIFTS of the asymmetric stretch of UiO-66 in air. **(d)** Modified van't Hoff plot of the asymmetric stretch of UiO-66 in air. X^{-1} denotes inverse flexibility constants [loose]/[tight]. Data were fitted to $X^{-1} = \exp[-(\Delta H + \Delta C_p(T - 298.15\ K) - T(\Delta S + \Delta C_p \ln(T/298.15\ K)))/RT]$.

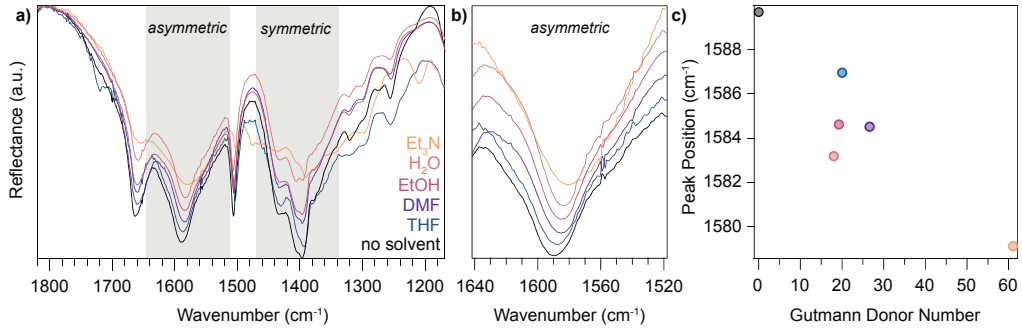

Figure 3*:* **(a)** Solvent-dependent VT-DRIFTS of UiO-66 displaying asymmetric and symmetric carboxylate stretch. **(b)** Highlighted portion of the spectra demonstrating the shift in the asymmetric stretch with each solvent. **(c)** Correlation plot between asymmetric stretch peak position versus Gutmann donor number for each solvent.

strongly implies the co-exist of two species in equilibrium and in nearly 1:1 mixtures at intermediate temperatures. Peak asymmetry across temperature ranges has been described in detail for other MOF systems by Andreeva and coworkers [7,8]. Rather than consider the exact metal-carboxylate configuration in the system, the equilibrium model estimates the population of two shallow potential energy surfaces that are more "tight" or "loose." Thus, fitting these spectra to a two-Gaussian model produces relative ratios of the "tight" and "loose" species, i.e., the flexibility constant, at each temperature. Global fitting examples are provided in the Supporting Information. Any Gaussian fit that was below an R^2 value of 0.990 was considered unsuitable and not used in the calculation of *X*. Flexibility constants (*X*) reflect the equilibrium ratio of the population of bound and unbound ([bound]/[unbound]) species for a given metal-ligand bond, in an analogous fashion to the definition of stability constants. We derive the inverse flexibility constant, X^{-1}, from the ratio [loose]/[tight] extracted from the relative population ratios through Gaussian fitting. **Figure 2b** plots X^{-1} versus temperature for UiO-66 under dynamic vacuum derived from the asymmetric carboxylate stretch. The room temperature value of X corresponds to $\ln X = 1.84$ which compares well to stability constants reported for molecular metal carboxylate species.[17] Consistent with our previous analysis of CuBTC, we interpreted these data using a modified van't Hoff plot intended for phase change systems,[18] due to the soft mode nature of these vibrations. This fitting produces an excellent agreement, with $\Delta H = 17$ kJ mol^{-1}, $\Delta S = 48$ J mol^{-1}, and $\Delta C_p = 80$ J mol^{-1} K^{-1}. Consistent with UiO-66 being chemically robust, it possesses larger flexibility constants and larger endothermic enthalpy barriers than reported previously for CuBTC or *M*(1,2,3-triazolate)$_2$ MOFs.[7,8] And yet, a ln*X* of 1.84 is lower than stability constants reported for coordination polymers, including metal-carbene and metal-pyridyl materials known to exhibit self-healing behavior.[20,21] As reference, a table of stability constants for these materials is provided in the SI Table S4). In comparison to the $\Delta S = 22.0$ J mol^{-1} K^{-1} of CuBTC the larger entropy term of UiO-66 suggests a bigger difference in the number of microstate metal-linker bond configurations between the "tight" and "loose" states, while the comparatively large ΔC_p implies that the conversion into the "loose" state involves more degrees of freedom than the corresponding process for CuBTC. Because MOF applications, ranging from gas separations to catalysis, involve the presence of guest molecules, we explored the metal-linker equilibrium in air. **Figure 2c** plots the baseline-subtracted asymmetric carboxylate stretch in air between 294 K – 473 K. Remarkably, the peak maxima redshift increases in slope from –0.015 to –0.051 cm^{-1} K^{-1}. This slope, the largest yet observed for a MOF, suggests the presence of guest molecules favor the "loose" state bond conformations. Evidence abounds that guest molecules, as innocuous as N_2, interact with MOF metal nodes.[22,23] Given the composition of air, we assume that the interaction involves water molecules and, to a lesser extent, CO_2 and N_2, which both possess large quadrupole moments,[24,25] and, hence, high polarizability. **Figure 2c** plots the shifting asymmetric stretch in the presence of air. To avoid moisture condensation, 300 K was the lowest temperature employed. Global fitting analysis of these data indicate that the presence of air favors the "loose" state more than in vacuum, with larger $\ln X^{-1}$ values observed at each temperature. The corresponding van't Hoff analysis produces $\Delta H = 15$ kJ mol^{-1}, $\Delta S = 32$ J mol^{-1}, and $\Delta C_p = 220$ J mol^{-1} K^{-1}. While the enthalpic barrier and entropic driving force are similar in magnitude, albeit smaller, than in vacuum, the change in specific heat is significantly larger. We propose that the bond equilibrium process involves greater degrees of freedom when in air, suggesting the participation of N_2, CO_2, and H_2O.

Given this evidence that UiO-66 metal-linker bonds destabilize in the presence of air, we explored the effect of solvent. Specifically, guest molecules were targeted for their Lewis and Brønsted basicity, given that the interaction with air likely involves water molecules associating to metal sites, promoting metal-linker bond weakening. **Figure 3** shows DRIFTS spectra of UiO-66 soaked with different solvents and collected at 298 K, with the evacuated material plotted for comparison. The addition of all solvents, Et_3N, H_2O (pH 7), EtOH, DMF, and THF, induced significant redshifts to both the asymmetric and symmetric peak maxima. Despite studies of UiO-66 structurally degrading under extremely basic/acidic conditions,[26] we observe the MOF retains crystallinity over a 3-hour time period exposed to Et_3N, which exceeds the duration of VT-DRIFTS data collection (Figure S6). Solvent-dependent stability constants have been reported previously, notably for multi-dentate ligands, with water being highly effective at promoting metal-ligand bond cleavage.[27] Gutmann donor numbers also provide a convenient metric for understanding the redshifting trends by quantifying Lewis basicity.[28] With the largest donor number, at 61, Et_3N likely promotes the "loose" state by attacking the Zr

centers. This microscopic picture is further demonstrated by the negative flexibility constant, ln*X*, for Et_3N, -0.61. The remaining solvents have donor numbers between ~20-30 whose flexibility constants scale with increasing donor number. **Figure 3c** illustrates the apparent correlation between the peak position of the asymmetric stretch and the donor number of the guest solvent. **Table 1** summarizes the solvent-dependence of UiO-66 metal-linker dynamics. The solvents that induce the greatest redshifts also cause the smallest flexibility constants, ln*X*. Remarkably, these data suggest strongly binding solvents, such as H_2O and Et_3N, destabilize MOF metal-linker bonding to such a degree that the loose states begin to dominate the coordination environments even at room temperature. We attribute the strong effect of water to its high molar volumetric density and its strong ability to engage in hydrogen bonding, to which the metal-oxide clusters of a MOF are highly susceptible.

Table 1: Environment-dependent flexibility constants at room temperature (ln*X* when *X* = [tight]/[loose] of the asymmetric carboxylate stretch in UiO-66.

Solvent	Asymmetric peak (cm^{-1})	ln*X* [asymmetric]
Vacuum	1589	1.8(4)
Air	1589	1.7(3)
N_2	1589	1.6(6)
THF	1587	1.3(9)
DMF	1585	0.85(8)
EtOH	1581	0.50(5)
H_2O	1579	0.04(0)
Et_3N	1577	-0.61(7)

In conclusion, through analysis of VT-DRIFTS and by fitting the spectra to a two-state equilibrium model of “tight” and “loose” bond conformations, flexibility constants, comparable with metal-linker stability constants of metal complexes, could be determined for UiO-66, the prototypical “stable” MOF. Employing a modified van’t Hoff analysis of these data suggests the chemical stability of UiO-66 and its higher stability constants arise from the “loose” state bearing similar bond enthalpies and entropies to the “tight” state favored at lower temperatures. These values are comparable to metal-carboxylate stability constants reported for molecular and polymeric materials and become more labile in the presence of gas-phase and liquid guest molecules. These results provide quantitative tools for rationalizing previous phenomena of MOFs and for harnessing their labile bonding.

Conflicts of interest

There are no conflicts to declare.

Acknowledgements

We gratefully acknowledge the University of Oregon for startup funds. This work made use of the CAMCOR facility of the Lorry I. Lokey Laboratories at the University of Oregon to perform VT-DRIFTS experiments. C.K.B. acknowledges the Research Corporation for Science Advancement (Cottrell Award). This material is based upon work supported by the Department of Energy through the Office of Basic Energy Sciences under grant no. DE-SC0022147. Contributions from A.J.M. were supported by the Department of Energy, Basic Energy Sciences under grant no. DE-SC0012446.

Notes and references

1 J. Hartwig, in *Organotransition Metal Chemistry: From Bonding to Catalysis*, 2010.
2 I. B. Bersuker, *The Jahn-Teller Effect and Vibronic Interactions in Modern Chemistry*, Springer US, Boston, MA, 1984.
3 G. Venkataraman, *Bull. Mater. Sci.*, 1979, **1**, 129–170.
4 C. Chakravarty, P. G. Debenedetti and F. H. Stillinger, *J. Chem. Phys.*, 2007, **126**, 204508.
5 A. M. A. Leguy, A. R. Goñi, J. M. Frost, J. Skelton, F. Brivio, X. Rodríguez-Martínez, O. J. Weber, A. Pallipurath, M. I. Alonso, M. Campoy-Quiles, M. T. Weller, J. Nelson, A. Walsh and P. R. F. Barnes, *Phys. Chem. Chem. Phys.*, 2016, **18**, 27051–27066.
6 F. Panzer, C. Li, T. Meier, A. Köhler and S. Huettner, *Adv. Energy Mater.*, 2017, **7**, 1–11.
7 A. B. Andreeva, K. N. Le, L. Chen, M. E. Kellman, C. H. Hendon and C. K. Brozek, *J. Am. Chem. Soc.*, 2020, **142**, 19291–19299.
8 A. B. Andreeva, K. N. Le, K. Kadota, S. Horike, C. H. Hendon and C. K. Brozek, *Chem. Mater.*, 2021, **33**, 8534–8545.
9 S. L. Gould, D. Tranchemontagne, O. M. Yaghi and M. A. Garcia-Garibay, *J. Am. Chem. Soc.*, 2008, **130**, 3246–3247.
10 Z. Liu, Y. Wang and M. A. Garcia-Garibay, *J. Phys. Chem. Lett.*, 2021, **12**, 5644–5648.
11 C. K. Brozek and M. Dincă, *Chem Sci*, 2012, **3**, 2110–2110.
12 C. K. Brozek and M. Dincă, *J. Am. Chem. Soc.*, 2013, **135**, 12886–12891.
13 C. K. Brozek and M. Dincă, *Chem. Soc. Rev.*, 2014, **43**, 5456.
14 K. Leus, I. Muylaert, M. Vandichel, G. B. Marin, M. Waroquier, V. Van Speybroeck and P. Van der Voort, *Chem. Commun. Camb. Engl.*, 2010, **46**, 5085–5087.
15 K. Leus, M. Vandichel, Y. Y. Liu, I. Muylaert, J. Musschoot, S. Pyl, H. Vrielinck, F. Callens, G. B. Marin, C. Detavernier, P. V. Wiper, Y. Z. Khimyak, M. Waroquier, V. Van Speybroeck and P. Van Der Voort, *J. Catal.*, 2012, **285**, 196.
16 M. D. Allendorf, V. Stavila, M. Witman, C. K. Brozek and C. H. Hendon, *J. Am. Chem. Soc.*, 2021, **143**, 6705–6723.
17 J. W. Bunting and K. M. Thong, *Can. J. Chem.*, 1970, **48**, 1654.
18 C. Y. Huang, T. Wang and F. Gai, *Chem. Phys. Lett.*, 2003, **371**, 731–738.
19 M. J. Katz, Z. J. Brown, Y. J. Colón, P. W. Siu, K. A. Scheidt, R. Q. Snurr, J. T. Hupp and O. K. Farha, *Chem. Commun.*, 2013, **49**, 9449.
20 R. Dobrawa and F. Würthner, *J. Polym. Sci. Part Polym. Chem.*, 2005, **43**, 4981–4995.
21 A. K. de K. Lewis, S. Caddick, F. G. N. Cloke, N. C. Billingham, P. B. Hitchcock and J. Leonard, *J. Am. Chem. Soc.*, 2003, **125**, 10066.
22 C. K. Brozek, A. Ozarowski, S. A. Stoian and M. Dincă, *Inorg Chem Front*, 2017, **4**, 782–788.
23 K. S. Walton and R. Q. Snurr, *J Am Chem Soc*, 2007, **129**, 8552.
24 A. D. Buckingham, 15.
25 A. D. Buckingham, R. L. Disch and D. A. Dunmur, *J. Am. Chem. Soc.*, 1968, **90**, 3104–3107.
26 D. Bůžek, J. Demel and K. Lang, *Inorg. Chem.*, 2018, **57**, 14290.
27 B. G. Cox, J. Garcia-Rosas and H. Schneider, *J. Am. Chem. Soc.*, 1981, **103**, 1384–1389.
28 V. Gutmann, *Coord. Chem. Rev.*, 1976, **18**, 225–255.

